Structural characterization of strained silicon grown on a SiGe buffer layer

2008 Semicond. Sci. Technol. 23 035012

(http://iopscience.iop.org/0268-1242/23/3/035012)

Semicond. Sci. Technol. **23** (2008) 035012 (5pp) doi:10.1088/0268-1242/23/3/035012

Structural characterization of strained silicon grown on a SiGe buffer layer

J H Jang[1], M S Phen[1], A Gerger[1], K S Jones[1], J L Hansen[2], A N Larsen[2] and V Craciun[1]

[1] Department of Materials Science and Engineering, University of Florida, 100 Rhines Hall, PO Box 116400, Gainesville, FL 32611-6400, USA
[2] Department of Physics and Astronomy, University of Aarhus, DK-8000 Aarhus, Denmark

E-mail: huse29@ufl.edu

Received 24 October 2007, in final form 9 January 2008
Published 7 February 2008
Online at stacks.iop.org/SST/23/035012

Abstract

The microstructure of about 50 nm thick strained-Si/$Si_{0.7}Ge_{0.3}$/graded-SiGe/Si-substrate layers grown by MBE (molecular beam epitaxy) was characterized using high-resolution x-ray based characterization techniques. The degree of relaxation of the Si-capping layer after a thermal anneal at 800 °C for 30 min was determined using reciprocal space map (RSM) scans recorded around the (1 1 3) diffraction plane. However, since a RSM is not suitable when the strain relaxation is very small, x-ray reflectivity (XRR) and omega rocking curves (ω-RCs) were employed for the relaxation study. XRR spectra were collected and analyzed to obtain thickness, Ge concentration and surface/interfacial roughness information of the as-grown and annealed samples. ω-RCs were performed in order to investigate the crystalline quality of the samples. It was found that the annealed strained layer showed higher Lorentzian fraction in ω-RCs and misfit defect density which were caused by strain relaxation. In addition, the results showed that after the annealing process the broadening in the tail region of the ω-RCs was indicative of a change in the coherence length distribution of the crystallite size. The misfit defects and surface morphology obtained from transmission electron microscopy (TEM) and atomic force microscopy (AFM) investigations were consistent with results obtained from the x-ray based characterization techniques.

1. Introduction

Over the past several decades, there has been an interest in strained-Si/SiGe/Si-substrate heterostructures because a change in band structure and density of states due to strain produces an enhancement in the mobility of charge carriers [1–3]. In an n-MOSFET device with channel regions formed by pseudomorphic growth of strained Si on a relaxed $Si_{0.7}Ge_{0.3}$ template, the effective electron mobility reached a 1010 $cm^2\ V^{-1}\ s^{-1}$ value [4], which is 80% higher than that of normal silicon (560 $cm^2\ V^{-1}\ s-1$). For this strain-based technology application, the strain relaxation and misfit/threading dislocations are key parameters. During the device processing, such as the post-growth annealing and ion implantation of a strained silicon layer, the strain begins to relax via the generation of defects, especially misfit/threading dislocations, and Ge interdiffusion, which degrade the device performance by decreasing the charge mobility and increasing the leakage current [5–8]. Since threading dislocations (TDs) have a major influence upon device performance, many alternative processes for reducing their density have been suggested [9, 10]. As the misfit dislocation density depends on the materials involved, it will be mainly determined by the lattice mismatch and different thermal coefficients rather than the growth condition due to its intrinsic nature. In contrast to the misfit dislocations, the threading dislocations primarily arise from the dislocated substrate/buffer layer and dislocation loops nucleated from the step edgy [11]. Therefore, the threading dislocation density can be reduced by alternative growth methods, such as an introduction of a graded buffer layer used in our study [12, 13]. These misfit/threading dislocations are primarily observed using transmission electron microscopy (TEM), which, unfortunately, has disadvantages such as complex and destructive sample preparation and it is time consuming. X-ray diffraction (XRD) could not only overcome

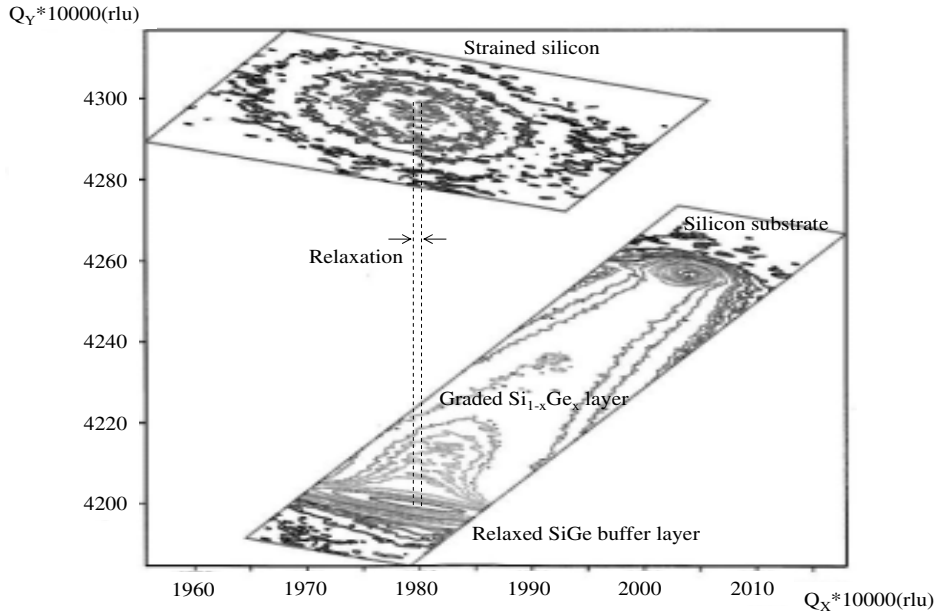

Figure 1. Reciprocal space map (1 1 3) of annealed strained-Si/$Si_{0.7}Ge_{0.3}$/graded-SiGe/Si-substrate.

these limitations by not requiring special sample preparation and being non-destructive, but also provide quantitative information about the sample. Therefore, our study focused on structural characterization of strained silicon layers by using high resolution x-ray characterization techniques for the better understanding of the defects generation due to strain relaxation.

2. Experiment details

A compositionally graded layer to confine threading dislocations was grown by gradually accommodating the lattice mismatch between $Si_{1-x}Ge_x$ layers [12, 13] on (1 0 0) silicon substrate via molecular beam epitaxy (MBE) in which the growth condition was shown in [14, 15]. A 630 nm thick layer of the fully relaxed $Si_{0.7}Ge_{0.3}$ was grown on top of the graded layer, followed by a 50 nm strained Si-capping layer. After growth, some of the strained samples were annealed at 800 °C for 30 min in the furnace to study how the temperature affects the microstructure of the strained layer. A PANanalytical MRD X'Pert system equipped with a mirror and a Ge (2 2 0) monochromator on the primary optics and a Ge (2 2 0) analyzer on the secondary optics was used to collect high-resolution x-ray diffraction rocking curves (RCs) and reciprocal space maps (RSM). For x-ray reflectivity (XRR) spectra, an x-ray mirror and parallel plate collimator were used as the primary and secondary optics, respectively. The scan conditions for all the samples were 0.002° step size and 10 s time per step for the ω-RCs and 0.005° and 3 s for XRR. In order to confirm the strain relaxation, misfit dislocations and surface morphology of the strained silicon layer, transmission electron microscopy (TEM) and atomic force microscopy (AFM) investigations were carried out on the JEOL TEM 200CX and Digital Instruments Nanoscope AFM setup under tapping mode, respectively.

3. Results and discussion

A typical high resolution reciprocal space map (RSM) recorded around the asymmetric (1 1 3) reflection from an annealed strained-Si/$Si_{0.7}Ge_{0.3}$/$Si_{1-x}Ge_x$/Si-substrate sample is shown in figure 1. This diffraction pattern is displayed as a function of scattering vector Q_X parallel and Q_Y perpendicular to the surface. From this RSM plot, several information regarding the sample structure can be extracted. First of all, it is found that the $Si_{0.7}Ge_{0.3}$ buffer layer is fully relaxed. If a buffer layer is relaxed and the thickness of strained silicon is less than the critical thickness, there is no driving force for the movement of the dislocations from the interface between the strained layer and relaxed buffer layer to the surface layer which indicates that misfit dislocations are not generated. As suggested by Loo *et al* [16], although the thickness of the strained silicon layer is below the critical thickness, thermal treatment can result in the formation of misfit dislocation originating at the heteroepitaxial interface between strained and buffer layers if the latter is not fully relaxed. The presence of the graded layer ($Si_{1-x}Ge_x$, with x from 0 to 0.3) between the Si-substrate and $Si_{0.7}Ge_{0.3}$ in which Ge was incorporated at a rate of 10 at% per micrometer on silicon substrates to composition of 30 at%Ge is clearly seen in figure 1. This continuous graded layer was employed for an effective reduction of threading dislocation density. Since the misfit dislocations in the graded layer are distributed homogeneously, the movement of the rather mobile threading dislocations will be blocked [17]. Finally, the topmost strained silicon peak appears to the upper left region of the silicon substrate peak. Since the peak width of the strained layer is very broad compared to Si-substrate or fully relaxed $Si_{0.7}Ge_{0.3}$, it can be expected that this broadening is due to defects, such as dislocations, and finite crystallite size. Also, the measured parallel and perpendicular mismatches between

Table 1. XRR simulation of the as-grown and annealed strained silicon samples. Relaxed SiGe buffer, interfacial, strained silicon and surface layers were applied as a sample model.

	As-grown strained silicon			Annealed strained silicon		
Layer	Thickness (Å)	Density (g cm^{-3})	Roughness (Å)	Thickness (Å)	Density (g cm^{-3})	Roughness (Å)
Buffer layer	–	3.40	3	–	3.40	2
Interfacial layer	15	2.69	23	15	2.91	26
Strained layer	530	2.33	7	533	2.31	15
Surface layer	5	2.13	44	6	2.14	47

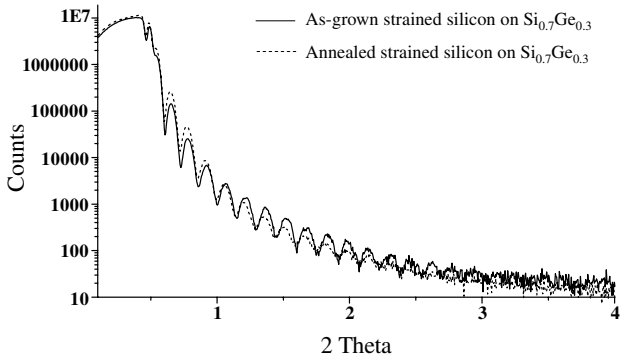

Figure 2. x-ray reflectivity (XRR) of the as-grown and annealed strained-Si/$Si_{0.7}Ge_{0.3}$/graded-SiGe/Si.

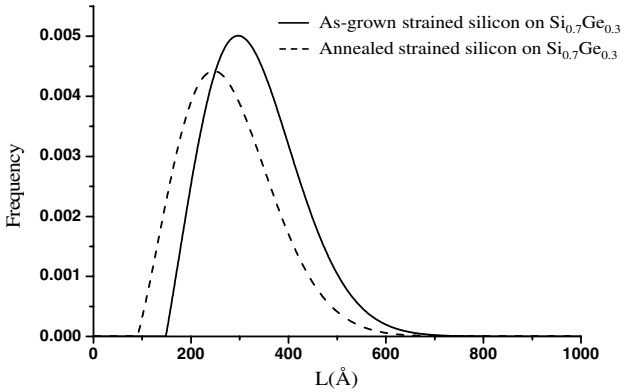

Figure 4. The coherence length distribution of the as-grown and annealed strained silicon. The length distribution function can be obtained from the second derivative of the Fourier size coefficient.

strained silicon and relaxed buffer layers are 1.01×10^{-3}% and 2.25%, respectively. The horizontal shift of the strained silicon with respect to the relaxed buffer layer is very small which indicates that there are two possibilities for the shift of that magnitude: (I) small strain relaxation due to post-growth annealing process and (II) presence of surface steps due to small wafer misorientation. Therefore, it is difficult to make an assertion whether a peak shift of the strained silicon layer with respect to the SiGe buffer layer is due to strain relaxation.

Figure 2 displays the x-ray reflectivity (XRR) spectra acquired from as-grown and annealed strained samples. Since x-ray reflectivity spectra were obtained using the symmetric $\theta/2\theta$ configuration with very small angles, this technique is suitable for the investigation and characterization of the thin film. The film density was determined by the critical angle (θ_c) in which the experimental deviation is about ±3% in our study. The non-spectra diffuse scattering as well as the specular scattering was considered in order to obtain the surface and interfacial roughness values. Figure 2 shows a different reflectivity of a thin film of as-grown and annealed strained Si deposited on a SiGe buffer layer, resulting from the effects of the strained layer's roughness and interfacial layer's density. Using the Wingixa® software from PANanalytical, one can get layer roughness, density and thickness values, which are listed in table 1. In the simulation of XRR spectra, a multi-layer model, which consists of the $Si_{1-x}Ge_x$ buffer,

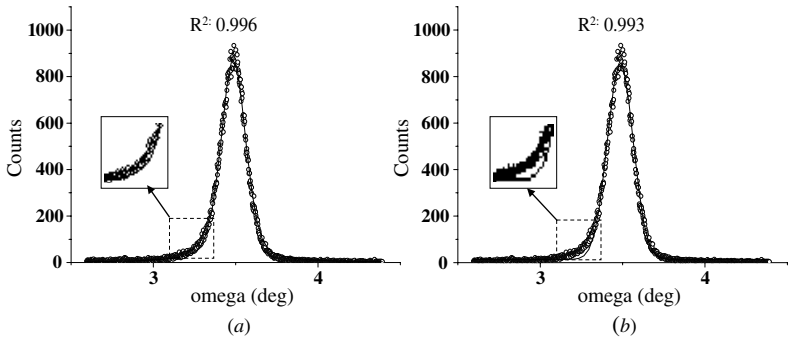

Figure 3. Curve fitting of (1 1 3) rocking curve of the annealed strained silicon using (*a*) pseudo-Voigt and (*b*) Gaussian functions. R^2 is a goodness of fit statistics which is the square of the correlation between the response values and the predicted response values.

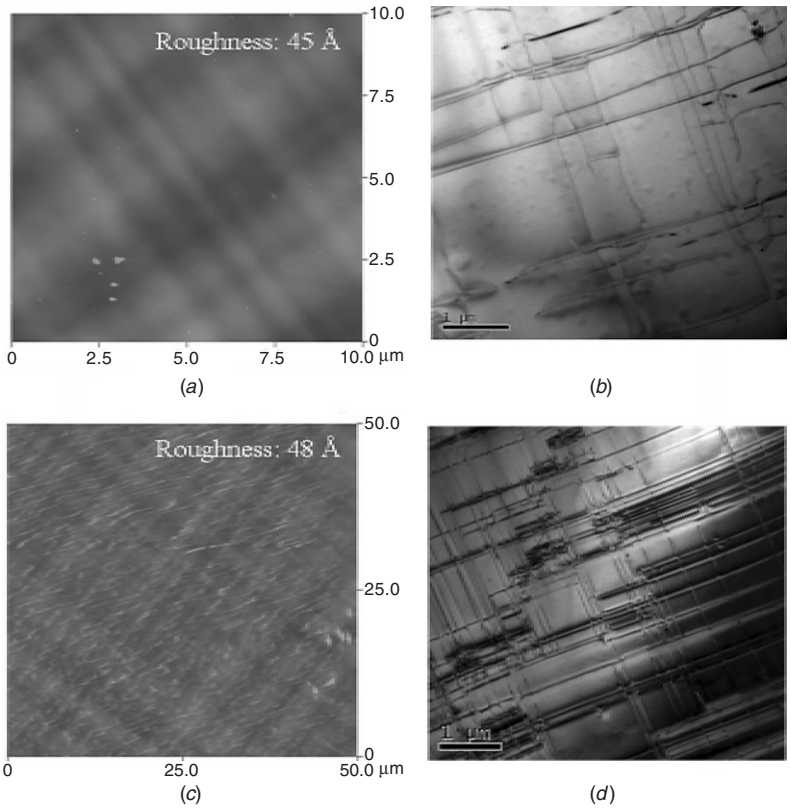

Figure 5. Atomic force microscopy (AFM) and transmission electron microscopy (TEM) images of as-grown (*a*) and (*b*) and annealed (*c*) and (*d*) strained silicon. AFM images were obtained under the tapping mode and TEM images under the bright field mode.

interfacial, strained silicon and surface layers, was used to obtain the best simulation. Estimated Ge composition of relaxed SiGe buffer layer is about 31–32% [18]. It is found in table 1 that the density of the interfacial layer and roughness of the strained layer in the annealed sample are higher than those in the as-grown sample. It appears that Ge atoms in the relaxed $Si_{0.7}Ge_{0.3}$ layer slightly diffused into the strained silicon layer and strain was relaxed during the post-growth annealing process [19].

Figure 3 shows a (1 1 3) omega rocking curve acquired from annealed strained Si, which is fitted with pseudo-Voigt and Gaussian functions. The former is a linear combination of a Lorentzian and a Gaussian function. For the best fit, a goodness of fit statistics (R^2) was also measured which is the square of the correlation between the response values and the predicted response values. It is clear that a pure Gaussian function does not fit well in the tail region of the diffraction profile because of the absence of a Lorentzian component. Therefore, a pseudo-Voigt function is more suitable to fit the RCs, as shown previously [20]. In this study, ω-RCs of (1 1 3), (0 0 4) and (2 2 4) planes were analyzed for the estimation of the full width at half maximum (FWHM). Notably, (1 1 3) and (2 2 4) planes require the case of grazing incidence angles, around 2.8° and 8.8°, respectively. This small incidence angle results in a large surface interaction volume, therefore being more sensitive to the surface layer. The RCs of the strained layers were fitted with Voigt and pseudo-Voigt functions in order to find out the diffraction line profile shape, as listed in table 2. It is found that while the RCs of as-grown strained silicon show almost pure Gaussian shape (W_L and η are close to 0), those of annealed strained silicon show Lorentzian as well as Gaussian shapes with higher fraction (η) of the Lorentzian component. It means that the annealing has a strong effect on the line broadening in the tail region of the RCs. Since the increase of FWHM values of annealed strained silicon is primarily associated with the dislocations, it is believed that the strain relaxation occurs during the high temperature anneal.

Table 2. The line profile analysis of the as-grown and annealed strained silicon. The diffraction profiles were fitted by Voigt and pseudo-Voigt functions.

		Voigt		Pseudo-Voigt	
		W_G[a]	W_L[b]	W_{Psd}[c]	η[d]
As-grown	(1 1 3)	0.151°	0.006°	0.154°	0.05
strained-Si/$Si_{0.7}Ge_{0.3}$	(0 0 4)	0.149°	∼0°	0.150°	∼0
	(2 2 4)	0.155°	∼0°	0.155°	∼0
Annealed	(1 1 3)	0.138°	0.066°	0.176°	0.46
strained-Si/$Si_{0.7}Ge_{0.3}$	(0 0 4)	0.131°	0.078°	0.177°	0.52
	(2 2 4)	0.150°	0.053°	0.179°	0.37

[a] W_G: FWHM of Gaussian function.
[b] W_L: FWHM of Lorentzian function.
[c] W_{Psd}: FWHM of pseudo-Voigt function.
[d] η: fraction of the Lorentzian component ($0 \leqslant \eta \leqslant 1$).

This result raised the question of what is the physical meaning of the tail part of the x-ray rocking curve. The tail part of the ω-RC is related to the finite coherence length which can be defined as an average crystallite size which scatters coherently in which the defects are free [21]. The coherence length can be statistically estimated by using Fourier analysis [22]. First of all, the Fourier coefficients of the diffraction line profile can be determined from the Gaussian and Lorentzian component of the Voigt function and then separated into size and mean squared strain coefficients which are expressed by following equations [23]:

$$A(L) = \exp\left(-2LW_{\mathrm{L}} - \pi L^2 W_{\mathrm{G}}^2\right) \quad (1)$$

$$A(L) = A_{\mathrm{S}}(L)\exp(-2\pi Q^2 L^2 \varepsilon^2), \quad (2)$$

where, $A(L)$ and $A_{\mathrm{S}}(L)$ are the Fourier and size coefficients, W_{L} and W_{G} are the FWHM of Lorentzian and Gaussian functions, L, Q and ε are the coherence length, reciprocal lattice spacing and strain, respectively. Finally, the coherence length distribution ($P(L)$) can be obtained from the second derivative of the size coefficient [24]. Figure 4 shows the coherence length distribution of annealed and as-grown strained silicon. It is found that the mean coherence length of annealed strained silicon is smaller than that of as-grown one due to the generation of misfit defects. Figure 5 shows the surface morphologies and plan-view images of the as-grown and annealed strained silicon obtained from AFM and TEM. The large-scale cross-hatching roughness characteristic and misfit defects are clearly shown in AFM and TEM images, respectively. We clearly see that the annealed strained silicon has more cross-hatching characteristics than the as-grown one due to strain relaxation, consistent with the results obtained from x-ray techniques.

4. Conclusions

In summary, annealed and as-grown strained silicon layers were characterized by using high resolution x-ray diffraction. Although the parallel mismatch between the annealed strain silicon and SiGe buffer layer in RSM was very small, the evidence given by XRR and ω-RC techniques manifested the strain relaxation during annealing process at 800 °C for 30 min. In addition, it was found that the coherence length of the strained silicon decreased under high temperature annealing, which induced a line broadening in the tail region of ω-RCs. The results indicate that XRR and ω-RC are more suitable techniques than RSM when the strain relaxation is small.

Acknowledgements

We would like to thank Major Analytical Instrumentation Center (MAIC) in University of Florida for the use of the PANanalytical MRD X'Pert system and JEOL TEM CX200.

References

[1] Chidambaram P R, Bowen C, Chakravarthi S, Machala C and Wise R 2006 *IEEE Trans. Electron Devices* **53** 944
[2] Rim K *et al* 2003 *Solid-State Electron.* **47** 1133
[3] Goo J-S *et al* 2003 *IEEE Electron Device Lett.* **24** 351
[4] Welser J, Hoyt J L and Gibbons J F 1994 *IEEE Electron Device Lett.* **15** 100
[5] Vyatkin A F *et al* 2000 *Ion Implantation Technol.* **1720** 70
[6] Lindgren A-C, Chen C, Zhang S-L, Ostling M, Zhang Y and Zhu D 2002 *J. Appl. Phys.* **91** 2708
[7] Ismail K 1996 *J. Vac. Sci. Technol.* B **14** 2776
[8] Fiorenza J G *et al* 2004 *Semicond. Sci. Technol.* **19** L4
[9] Giovane L M, Luan H C, Agarwal A M and Kimerling L C 2001 *Appl. Phys. Lett.* **78** 541
[10] Jain S C, Osten H J, Dietrich B and Rucker H 1995 *Semicond. Sci. Technol.* **10** 1289
[11] Mahajan S and Sree Harsha K S 1998 *Principles of Growth and Processing of Semiconductors* (New York: McGraw-Hill)
[12] Olsen S H, O'Neill A G, Chattopadhyay S, Kwa K S, Driscoll L S, Norris D J, Cullis A G, Robbins D J and Zhang J 2004 *Semicond. Sci. Technol.* **19** 707
[13] Yuan X L, Sekiguchi T, Niitsuma J, Sakuma Y, Ito S and Ri S G 2005 *Appl. Phys. Lett.* **86** 162102
[14] Fitzgerald E A, Xie Y-H, Green M L, Brasen D, Kortan A R, Michel J, Mii Y-J and Weir B E 1991 *Appl. Phys. Lett.* **59** 811
[15] Phen M S, Crosby R T, Jones K S, Law M E, Hansen J L and Larsen A N 2005 *Mater. Res. Soc. Symp. Proc.* **864**
[16] Loo R, Delhougne R, Caymax M and Ries M 2005 *Appl. Phys. Lett.* **87** 182108
[17] Romanov A E, Pompe W, Mathis S, Beltz G E and Speck J S 1999 *J. Appl. Phys.* **85** 182
[18] Schaffler F 1997 *Semicond. Sci. Technol.* **12** 1515
[19] Wong L H, Wong C C, Ong K K, Liu J P, Chan L, Rao R, Pey K L, Liu L and Shen Z X 2004 *Thin Solid Films* **462–3** 76
[20] Young R A and Wiles D B 1982 *J. Appl. Cryst.* **15** 430
[21] Chierchia R, Bottcher T, Heinke H, Einfeldt S, Figge S and Hommel D 2003 *J. Appl. Phys.* **93** 8918
[22] Warren B E and Averbach B L 1950 *J. Appl. Phys.* **21** 595
[23] Boulle A, Legrand C, Guinebretiere R, Mercurio J P and Dauger A 2001 *Thin Solid Films* **391** 42
[24] Bertaut E F 1950 *Acta Cryst.* **3** 14